The College of Engineering
University of Wisconsin-Madison

Wisconsin Electric Machines and Power Electronics Consortium

RESEARCH REPORT
88-30

Simulation of Inverter Fed Induction Motors Including Core Losses

M.R. Udayagiri
Central Electronics Engineering
Research Institute
Pilani, 333031 INDIA

Thomas A. Lipo
Dept. of Electrical & Computer Engrg.
University of Wisconsin-Madison
1415 Johnson Drive
Madison, WI 53706-1691

WEMPEC

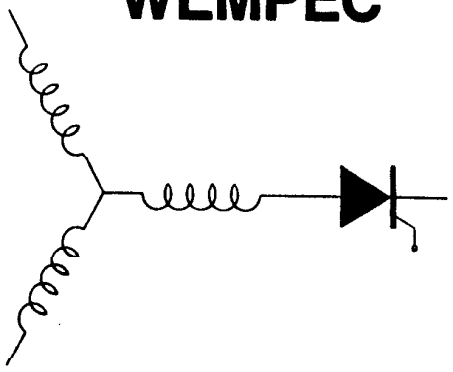

Department of Electrical and Computer Engineering
1415 Johnson Drive
Madison, Wisconsin 53706

SIMULATION OF INVERTER FED INDUCTION MOTORS INCLUDING CORE LOSSES

M.R. UDAYAGIRI
Central Electronics Engineering
Research Institute
Pilani, 333031 INDIA

THOMAS A. LIPO
University of Wisconsin
Dept. of Elect. and Comp. Engr
Madison WI, U.S.A.

Abstract This paper concerns the development of a simulation model for an induction motor including both eddy current losses and hysteresis losses. Since both eddy current loss and hysteresis loss are frequency dependent a new induction motor model with stator and rotor circuits expressed in different reference frames is presented in the paper to facilitate analysis. As the nature of the eddy current and hysteresis losses are ohmic, the stator and rotor eddy current losses can be represented by resistors across the stator and rotor magnetizing inductances. Necessary equations are derived to calculate the values of these resistors.

INTRODUCTION

Recent achievements in high power semiconductor device technology on one hand and custom built microcircuits on the other have widely increased the use of variable speed induction motor drive systems. Many sophisticated control strategies have been discussed in literature to improve the overall performance and efficiency of the system. Simulation of induction motors under steady state as well as dynamic conditions play an important role in the development of such systems. At present, the induction motor is simulated with attention paid only to the stator and rotor copper losses. However, this loss component frequently accounts for typically only two thirds of the losses in the machine. With the increased importance given to the performance and efficiency of the variable speed drive systems, it becomes increasingly important to have available induction motor models which include all the motor losses.

The conventional model of induction motor suggested by various authors in literature is suitable only for calculating the copper losses in the stator and rotor windings. Sufficient literature is available for catering to the deep bar effect in the rotor bars to exactly calculate the copper losses. Articles dealing with the simulation of induction motor have, until now, either neglected the core losses in the model or represented the losses with an approximate constant value resistor across the magnetizing inductance of the equivalent circuit. However, in order to develop variable speed AC motor drives with efficiency improvement, for example, these losses must be represented as exactly as possible so as to have a reliable simulation and hence good performance of the resulting hardware. A more accurate iron loss model of an induction motor for use in simulation studies is the subject of this paper.

EQUIVALENT CIRCUIT DEVELOPMENT OF SQUIRREL CAGE INDUCTION MOTOR WITH CORE LOSSES

In general, core losses arise both due to the induced currents in the core as well as the hysteresis characteristics of the core material. If the magnetic field set up in a ferromagnetic core is time varying, the field will induce a voltage in the core and thus cause current flow within the core itself. Due to the finite resistance of the core material, a resulting power loss occurs. As the thickness of the lamination used in the core is generally very small in comparison with the other dimensions of either stator or rotor core of the machine, it is convenient to assume that flux is uniform throughout the lamination. It is not difficult to show that the instantaneous power loss (eddy current loss) of the stator or rotor core per phase is then,

$$P_e(t) = \frac{V^* w^2 * N_e}{12\rho * N^2 * A^2 * m} v_\phi(t)^2 \qquad (1)$$

where $v_\phi(t)$ = instantaneous voltage across the winding exciting the core
V = volume of one lamination
w = thickness of the lamination
N_e = number of laminations in the core
ρ = resistivity of the lamination material
N = number of turns in the exciting winding
A = area of cross section perpendicular to the induced current.
m = number of phases

If the eddy current loss is represented as an ohmic loss in a resistor R_e which is in parallel with the core, then:

$$P_e(t) = \frac{v_\phi(t)^2}{R_e} \qquad (2)$$

$$\text{where } R_e = \frac{12\,\rho N^2 A^2 m}{V_l * w^2 * N_e} \qquad (3)$$

It is interesting to note that Eq. 1 is independent of both waveform and frequency and can therefore be conveniently used with inverter waveforms as well as for sinusoidal excitation.

As the hysteresis loss (P_h) in a core is essentially proportional to the area of the hysteresis loop of the core material, the hysteresis loss can be represented as:

$$P_h = k_h \int i \, d\lambda \qquad (4)$$

However, since

$$\lambda = Li$$

$$P_h = k_h L \int i \, di = k_h \frac{1}{2} L i^2 \qquad (5)$$

From fundamental principles, the reactive power (P_x) developed in an inductance " L" by an AC current " i " at a frequency " f " is clearly given by :

$$P_x = \pi f L i^2 \qquad (6)$$

or

$$L^* P_x = \pi f L^2 i^2 = \pi f N^2 A^2 B^2(t) \qquad (7)$$

or

$$\frac{k_h \eta V P_x}{\pi N^2 A^2} = \eta k_h f B^2(t) = P_h \qquad (8)$$

where

P_h = hysteresis loss
$B(t)$ = flux density

and η = Steinmetz's constant

Equation 8 is simply the hysteresis loss (P_h) as obtained by Steinmetz's expression. In q and d axis components the reactive power is

$$P_x = \frac{3(v_q * i_d - v_d * i_q)}{2} \quad (9)$$

$$P_h = \frac{3 k_h \eta L}{2\pi N^2 A^2} (v_q i_d - v_d i_q) \quad (10)$$

Eq. 10 can also be expressed as

$$P_h = (3,2) \left(\frac{v_q^2}{R_q} - \frac{v_d^2}{R_d} \right) \quad (11)$$

where $$R_q = \frac{v_q}{i_d} * \frac{\pi N^2 A^2}{k_h \eta L} \quad (12)$$

and $$R_d = \frac{v_d}{i_q} * \frac{\pi N^2 A^2}{k_h \eta L} \quad (13)$$

Thus, the hysteresis loss can be expressed as an ohmic loss across equivalent resistors R_q and R_d. It is again interesting to note that Eq. 10 is independent of frequency and wave shape and can conveniently be used in the simulation of inverter fed induction machines. However, it is important to mention that only the major hysteresis loop has been accounted for so that losses due to minor loops produced by the inverter harmonics will not be properly taken into account. Also, minor loops produced by the slot openings are neglected so that the stray load loss component of iron losses is not included. An effort to provide answers to these questions is continuing at the University of Wisconsin.

When the induction motor stator frequency remains constant the rotor frequency depends on the rotor speed or slip. Since both the eddy current losses and hysteresis losses are frequency dependent it is convenient to have separate equivalent circuits for the stator and rotor so as to properly represent the frequency dependent effects which are clearly different on the two members. Another main advantage by having this type of circuit is that the stator can be simulated in an arbitrary reference frame which is stationary and the rotor can be simulated in another arbitrary reference frame which is rotating at rotor speed so as to eliminate completely the speed voltage terms. Figure 1 shows the proposed new q-d equivalent circuits for simulating the induction motor. Note that the stator and rotor are coupled through an ideal transformer. The ohmic losses in the resistors R_{es} and R_{er} represent the eddy current losses of the stator and rotor.

From Eq. 4, the hysteresis loss in the rotor can be calculated as

$$P_{hr} = k_h \int (i_{qr} * d\lambda_{qr} + i_{dr} * d\lambda_{dr}) \quad (15)$$

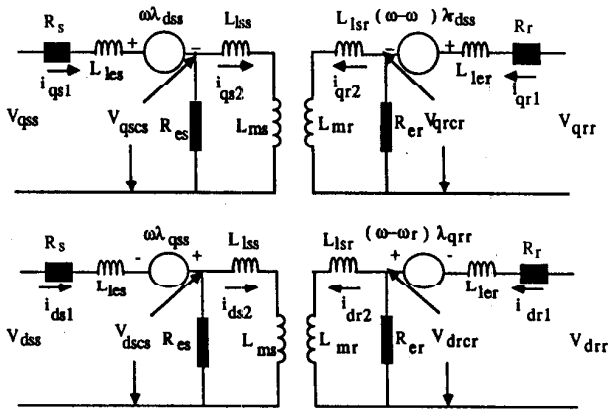

Fig. 1 q and d Axis Equivalent Circuits of Induction Motor In Arbitrary Reference Frame

or

$$P_{rh} = k_h \int (i_{qr} * \frac{d\lambda_{qr}}{dt} + i_{dr} * \frac{d\lambda_{dr}}{dt}) \, dt$$

From Fig.1 (16)

$$\frac{d\lambda_{qr}}{dt} = -R_r * i_{qr} - (\omega - \omega_r) \lambda_{dr} \quad (17)$$

and

$$\frac{d\lambda_{dr}}{dt} = -R_r * i_{dr} + (\omega - \omega_r) \lambda_{qr} \quad (18)$$

hence

$$P_{rh} = k_h [- \int i_{qr}^2 R_r \, dt - \int i_{dr}^2 R_r \, dt$$

$$- \int i_{qr} (\omega - \omega_r) \lambda_{dr} \, dt + \int i_{dr} (\omega - \omega_r) \lambda_{qr} \, dt] \quad (19)$$

If the rotor circuit is considered in stationary frame

$$P_{rh} = k_h [- \int i_{qr}^2 R_r \, dt - \int i_{dr}^2 R_r \, dt$$

$$+ \int i_{qr} \omega_r \lambda_{dr} \, dt - \int i_{dr} \omega_r \lambda_{qr} \, dt] \quad (20)$$

In Eq. 20 first two terms of the right hand side expression are always negative, as $i_{qr}^2 R_r$ and $i_{dr}^2 R_r$ are always positive. From Fig. 2 it can be observed that i_{qr} and λ_{dr} are out of phase and hence $i_{qr} \omega_r \lambda_{dr}$ will always be negative and that i_{dr} and λ_{qr} are in phase and hence $-i_{dr} \omega_r \lambda_{qr}$ will always be negative. Hence P_{rh} will always be negative. If the rotor circuit is considered in rotating frame which is rotating with rotor speed then:

$$P_{rh} \alpha [- \int i_{qr}^2 R_r \, dt - \int i_{dr}^2 R_r \, dt \quad (21)$$

and P_{rh} will always be negative. It is clear that the hysteresis loss in the rotor core of a squirrel cage induction motor cannot be negative and hence the model needs modification. As the hysteresis loss is only due to the hysteresis characteristics of the core, the reactive power absorbed by the core will be proportional to the hysteresis losses in the core. Hence it is necessary to represent the stator and rotor core separately in the equivalent circuits.

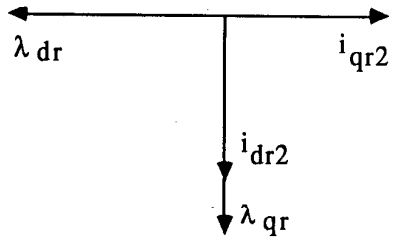

Fig. 2 Vector Diagram of Rotor Currents and Flux Linkages.

Figure 3 shows the modified q and d axis equivalent circuits when the stator is considered in stationary frame and the rotor in rotating frame which is rotating with rotor speed. As the core inductances are shown separately in Fig. 3 the reactive power consumed by these inductances should represent the hysteresis losses in the stator and rotor core. The eddy current loss resistors are also shown in Fig. 3 for completeness.

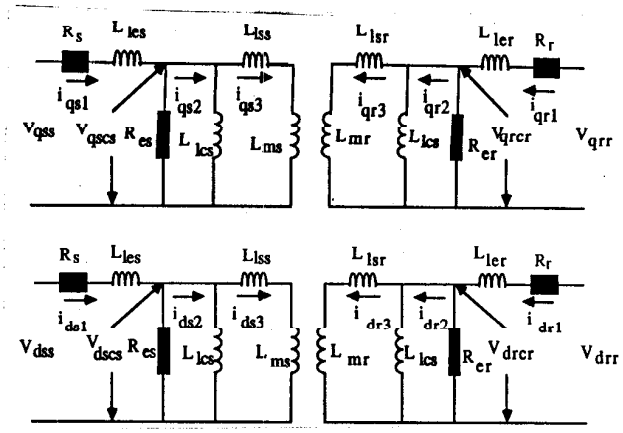

Fig. 3 q and d Axis Equivalent Circuits of Induction Motor with Core Losses. Stator Equations in Stationary Reference Frame, Rotor Equations in Rotor Reference Frame.

SIMULATION OF SQUIRREL CAGE INDUCTION MOTOR WITH CORE LOSSES:

From Fig.3 the following expressions can be derived:

$$\lambda_{qss} = \int (v_{qss} - i_{qs1} r_s - v_{qscs})\, dt \tag{22}$$

Since v_{qrr} is equal to zero for squirrel cage induction motor

$$\lambda_{qrr} = \int (-i_{qr1} r_r - v_{qrcr}) dt \tag{23}$$

hence

$$i_{qs1} = \frac{\lambda_{qss}}{L_{les}} \tag{24}$$

and

$$i_{qr1} = \frac{\lambda_{qrr}}{L_{ler}} \tag{25}$$

$$v_{qscs} = R_{se} (i_{qs1} - i_{qs2}) \tag{26}$$

$$v_{qrcr} = R_{re} (i_{qr1} - i_{qr2}) \tag{27}$$

$$\lambda_{qscs} = (i_{qs2} - i_{qs3}) L_{lcs} \tag{28}$$

$$\lambda_{qrcr} = (i_{qr2} - i_{qr3}) L_{lcr} \tag{29}$$

The flux linkages λ_{qscs} and λ_{qrcr} can also be expressed as

$$\lambda_{qscs} = \int (V_{qscs})\, dt \tag{30}$$

$$\lambda_{qrcr} = \int (V_{qrcr})\, dt \tag{31}$$

These flux linkages are also equal to

$$\lambda_{qscs} = L_{lss} * i_{qs3} + L_{ms} (i_{qs3} + i_{qr3s}) \tag{32}$$

$$\lambda_{qrcr} = L_{lsr} * i_{qr3} + L_{mr} (i_{qr3} + i_{qs3r}) \tag{33}$$

where

i_{qr3s} = q axis rotor current referred to stator frame

i_{qs3r} = q axis stator current referred to rotor frame

or

$$\lambda_{qscs} = i_{qs3} * L_{lss} + \lambda_{mqss} \tag{34}$$

$$\lambda_{qrcr} = i_{qr3} * L_{lss} + \lambda_{mqrr} \tag{35}$$

where

$$\lambda_{mqss} = L_{ms} (i_{qs3} + i_{qr3s}) \tag{36}$$

$$\lambda_{mqrr} = L_{mr} (i_{qr3} + i_{qs3r}) \tag{37}$$

From Eqs. 34 and 35,

$$i_{qs3} = \frac{\lambda_{qscs} - \lambda_{mqss}}{L_{lss}} \tag{38}$$

$$i_{qr3} = \frac{\lambda_{qrcr} - \lambda_{mqrr}}{L_{lsr}} \tag{39}$$

By substituting the values of i_{qs3} and i_{qr3} from Eqs.38 and 39 in Eqs.28 and 29

$$i_{qs2} = \frac{\lambda_{qscs} (L_{lss} + L_{lcs})}{(L_{lss} * L_{lcs})} - \frac{\lambda_{mqss}}{L_{lss}} \tag{40}$$

$$i_{qr2} = \frac{\lambda_{qrcr} (L_{lsr} + L_{lcr})}{(L_{lsr} * L_{lcr})} - \frac{\lambda_{mqrr}}{L_{lsr}} \tag{41}$$

From Eq. 39 if i_{qr3} is referred to stator frame then

$$i_{qr3s} = \frac{\lambda_{qrcs} - \lambda_{mqrs}}{L_{lsr}} \tag{42}$$

where $i_{qr3s} = i_{qr3}$ is referred to stator frame

$\lambda_{qrcs} = \lambda_{qrcr}$ referred to stator frame

and $\lambda_{mqrs} = \lambda_{mqrr}$ referred to stator frame

Substituting the values of i_{qs3} and i_{qr3s} from Eqs. 38 and 42 in Eq. 36:

$$\lambda_{mqss} + \frac{L_{ms}}{L_{lss}} \lambda_{mqss} + \frac{L_{ms}}{L_{lsr}} \lambda_{mqrs} = \frac{L_{ms}}{L_{lss}} \lambda_{qscs} + \frac{L_{ms}}{L_{lsr}} \lambda_{qrcs} \tag{43}$$

but $\lambda_{mqss} = L_{ms} (i_{qs3} + i_{qr3s})$

and $\lambda_{mqrs} = L_{mr} (i_{qr3s} + i_{qs3})$

hence

$$\lambda_{mqrs} = \frac{L_{mr}}{L_{ms}} \lambda_{mqss} \tag{44}$$

Substituting the value of λ_{mqrs} from Eq. 44 in Eq. 43 we have

$$\lambda_{mqss} = \frac{L_{ms}}{a * L_{lss}} \lambda_{qscs} + \frac{L_{ms}}{a * L_{lsr}} \lambda_{qrcs} \tag{45}$$

where $a = 1 + \frac{L_{ms}}{L_{lss}} + \frac{L_{mr}}{L_{lsr}}$

Similarly, $\lambda_{mqrr} = \frac{L_{mr}}{a * L_{lss}} \lambda_{qscr} + \frac{L_{mr}}{a * L_{lsr}} \lambda_{qrcr}$ (46)

where $\lambda_{qscr} = \lambda_{qscs}$ are referred to the rotor frame

Similar expressions for the d-axis circuit can be obtained from Fig. 3. By properly performing the transformation from stationary frame to rotating frame and vice-versa for the required quantities in the above equations, all the motor currents can be computed and the induction motor simulation therefore implemented.

As the core inductance is shown separately, the reactive power across the core inductances can be computed using the following expressions which are proportional to the hysteresis losses. For exact calculation of the hysteresis losses a proper scale factor should be used as already discussed.

$$P_{hs} = k_h V_{qscs} * (i_{ds2} - i_{ds3}) - V_{dscs} * (i_{qs2} - i_{qs3}) \tag{47}$$

and $$P_{hr} = k_h V_{qrcr} * (i_{dr2} - i_{dr3}) - V_{drcr} * (i_{qr2} - i_{qr3}) \tag{48}$$

The eddy current losses of stator and rotor can be computed using the following expressions:

$$P_{es} = 1.5 \frac{V_{qscs}^2 + V_{dscs}^2}{R_{se}} \tag{49}$$

and

$$P_{er} = 1.5 \frac{V_{qrcr}^2 + V_{drcr}^2}{R_{re}} \tag{50}$$

The copper losses can be computed using the following conventional expressions:

$$P_{cus} = 1.5 * R_s * (i_{qs1}^2 + i_{ds1}^2) \tag{51}$$

and

$$P_{cur} = 1.5 * R_r * (i_{qr1}^2 + i_{dr1}^2) \tag{52}$$

SIMULATION RESULTS FOR 250 HP SQUIRREL CAGE INDUCTION MOTOR

Using the above equations a 250 HP squirrel cage induction motor whose necessary and relevant parameters are given in Appendix 1 is simulated. The nature of the core losses can be predicted for a motor starting from zero speed to full speed in free acceleration mode without load. As the stator frequency is constant

for a particular supply frequency operation, the stator core losses (P_{es} and P_{hs}) should be independent of frequency for that particular case. At the starting instant, as the starting current is high, the drop across the stator circuit will be increased which results in less voltage across core and hence less stator core losses. As the motor picks up speed the input current and hence the stator drop decreases resulting in more voltage across the core. Thus, during this period stator core losses gradually increase and finally remains almost constant as the motor reaches steady state condition. Depending on the load conditions as the stator drop varies these losses also varies. As the rotor frequency f_r decreases from stator frequency f at the start to zero as the motor picks up speed, the rotor core losses (P_{er} and P_{hr}) decrease from maximum to minimum value. Depending on load conditions as the rotor speed and hence the rotor frequency varies the rotor eddy current losses also vary accordingly.

Figure 4 shows the torque and speed characteristics of the 250 HP squirrel cage induction motor with above method with sine wave input source in free acceleration mode under no load condition. Fig.5 (a), Fig.5(b) and Fig.5(c) show the stator and rotor eddy current losses, hysteresis losses and copper losses with sine wave input at 60 Hz. The results are in agreement with conventional steady state theory. In Fig. 6 the same model is used with a PWM inverter and the figure shows the resulting stator and rotor eddy current losses. It is interesting to note that the eddy current losses are pulsating in nature and reaching zero instantaneous values. According to definition of the eddy current losses, these losses are due to voltage induced in the core and as the input source is PWM, the induced voltages will have a PWM wave shape. Figure 7 shows the simulated current flowing through the eddy current loss resistor.

In order to further observe the validity of the model, the 250 HP motor is simulated with PWM inverter with 30 Hz input source with suitable input voltage so as to have constant v/f ratio. Fig.8 shows the torque and speed characteristics. Fig.9 shows the stator and rotor hysteresis losses with 30 Hz PWM input source to the motor.

CONCLUSIONS:

The paper has been concerned with the development of a reliable model for the squirrel cage induction motor which includes the effects of core losses. As the core is represented separately in the model, the saturation effects of the core may also be readily incorporated. If desired the model can also incorporate skin effect in the rotor bars. Using the developed model and simulation equations, a simulation of a 250 HP squirrel cage induction motor was implemented and the results were presented. This model is particularly suitable as a building block to generate a suitable PWM pattern which will have minimum motor losses. The model can also be used in adaptive control of variable frequency induction motor drives for improving the overall efficiency. Work on these subjects are in progress at CEERI, Pilani and UW-Madison.

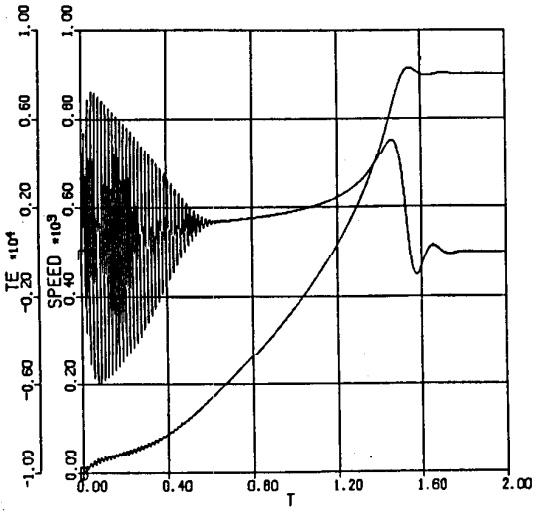

Fig. 4 Torque and Speed Characteristics of 250 HP Squirrel Cage Induction Motor.

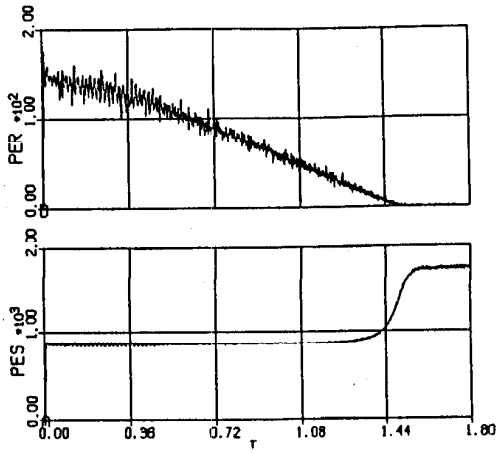

(a) Stator and Rotor Eddy Current Losses

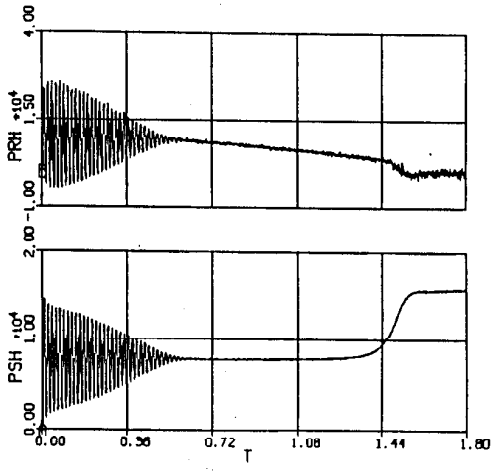

(b) Stator and Rotor Hysteresis Losses

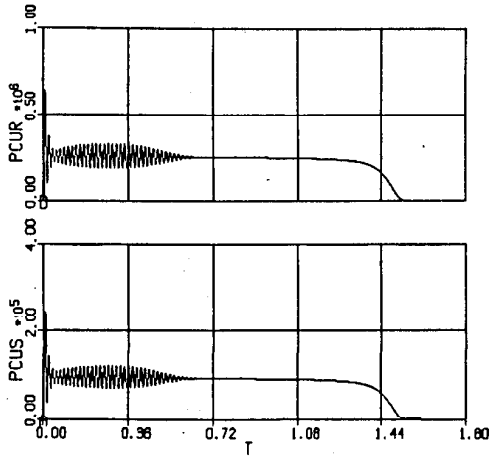

(c) Stator and Rotor Copper Losses

Fig. 5 Stator and Rotor Losses of 250 HP Induction During Free Acceleration with Sine Wave 60 Hz Excitation.

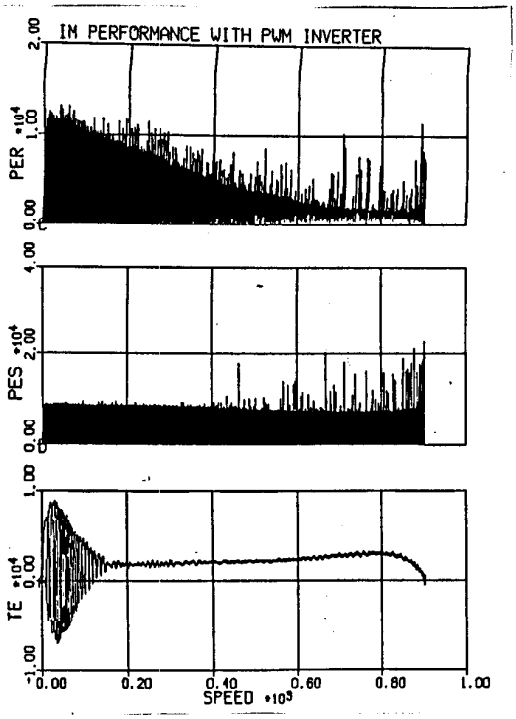

Fig.6. Stator and Rotor Eddy Current Losses with PWM Inverter.

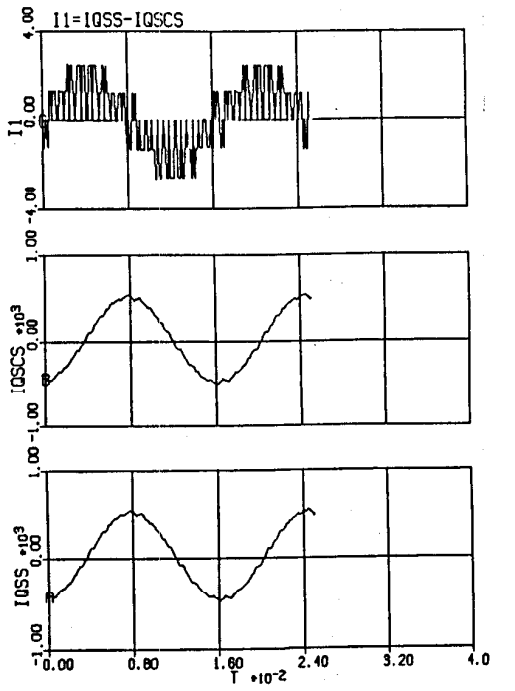

Fig.7. Eddy Current Loss Resistor Current with PWM Inverter.

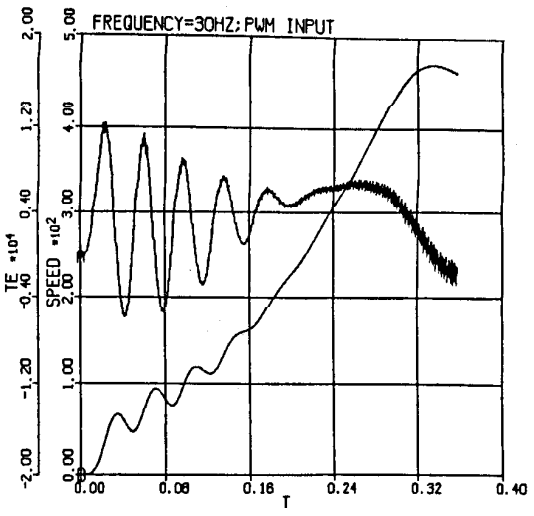

Fig.8. Torque and Speed Characteristics of 250 HP motor with 30 Hz PWM Inverter.

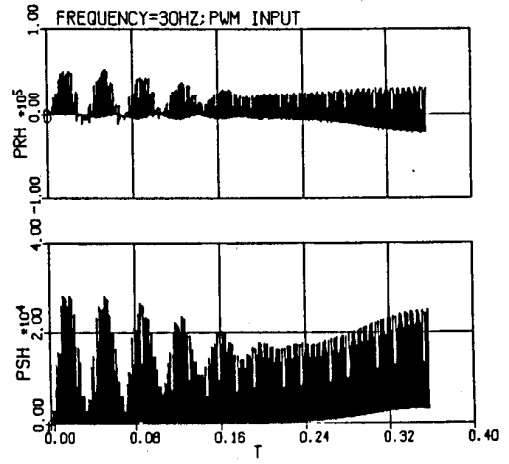

Fig.9. Stator and Rotor Hysteresis Losses with 30 Hz PWM Inverter.

ACKNOWLEDGMENTS

The authors wish to thank the authorities of Central Electronics Engineering Research Institute, PILANI (Rajasthan) INDIA; and the University of Wisconsin-Madison (WI) USA for allowing us to publish this work. The authors also like to thank for the financial assistance provided by the United Nations Development Program (UNDP).

REFERENCES:

1. P.C. Krause and C.H. Thomas,"Simulation of Symmetrical Induction Machinery",IEEE Transactions on Power Apparatus and Systems. Vol. PAS - 84, No 11, pp. 1038-1053.
2. L. J. Jacovides, "Analysis of Induction Motor Drives with a Non Sinusoidal Supply Voltage using Fourier Analysis", in Conf. Rec. of Fifth Annual meeting of IEEE IGA 1970, pp. 467-475.
3. F.G.G.De Buck; P. Gistelinck and D. De Backer, "A Simple but Reliable Loss model for Inverter - Supplied Induction Motors", IEEE Transactions on Industry Applications. Vol. IA-20; No.1; Jan/Feb 1984, pp. 190-202.
4. E. A. Klingshirn and H. E. Jordan. "Simulation of Poly Phase Induction Machines with Deep Bars", IEEE Transactions on Power Apparatus and Systems. Vol. PAS - 89; July/Aug 1970, pp. 1038-1043.
5. V. Gourishankar and D. H. Kelly, Electro Mechanical Energy Conversion (book), Intext Educational Publishers - New York 1973.

6. R.Bourne, Electrical Rotating Machine Testing, (book) London ILIFFE Books Ltd - 1970
7. T.A.Lipo and D.W.Novotny, "Dynamics and Control of AC Drives", Class Notes for ECE 711, University of Wisconsin - Madison.
8. T.A.Lipo, "Electromagnetic Design of AC Machines", Class Notes for ECE 713, University of Wisconsin - Madison.
9. J. O. Ojo, "Saturation Effects in Alternating Current Electric Machines" Ph.D Thesis, University of Wisconsin-Madison 1987.

APPENDIX

The following are the required design data and parameters of 250 HP, 8 pole, 2400 volts, 60 Hz Squirrel cage induction motor :

Stator outer diameter =	D_{os}	=	32 inches
Stator inner diameter=	D_{is}	=	24.08 inches
Rotor outer diameter =	D_{or}	=	24 inches
Rotor inner diameter=	D_{ir}	=	17.5 inches
Number of stator slots=	S_1	=	120
Number of rotor slots=	S_2	=	97
Gross core length=	l	=	10 inches
Lamination thickness=	w	=	0.025 inch
Type of steel			=2.6 % silicon steel
Length of stator and rotor stack=l_{is}=l_{ir}=			8.5 inches

Stator resistance=	R_s	=0.3347 ohms
Stator end ring leakage inductance=	L_{les}	=3.6012 mh
Stator core leakage inductance=	L_{lcs}	= 9.909 h
Stator slot leakage inductance=	L_{lss}	=3.6418 mh
Stator magnetizing inductance=	L_{ms}	= 0.3363 h
Stator eddy current loss resistance=	R_{es}	=3.26 K ohms
Rotor resistance=	R_r	=0.9192 ohms
Rotor end ring leakage inductance=	L_{ler}	=9.6656 mh
Rotor core leakage inductance=	L_{lcr}	= 13.5 h
Rotor slot leakage inductance=	L_{lsr}	=1.71 mh
Rotor magnetizing inductance=	L_{mr}	= 0.8078 h
Rotor eddy current loss resistance=	R_{er}	=25.0 K ohms